11th International Conference on Vibration Problems
Z. Dimitrovová *et al.* (eds.)
Lisbon, Portugal, 9-12 September 2013

STOCHASTIC BIFURCATION CHARACTERISTICS OF PZT-SMA COMPOSITE ENERGY HARVESTER

J. Xu*[1], M. Y. Luan[2], Z. W. Zhu[2]

[1] Tianjin Key Laboratory of Nonlinear Dynamics and Chaos Control
xujia_ld@163.com, mingyiluan@163.com

[2] Department of Mechanics, Tianjin University
zhuzhiwentju@163.com

Keywords: Piezoelectric Ceramics, Shape Memory Alloy, Composite Cantilever Beam, Stochastic Hopf Bifurcation.

Abstract. *A kind of PZT-SMA composite cantilever energy harvester was proposed in this paper, and its stochastic bifurcation characteristics were studied. SMA was chosen as the substrate of cantilever beam to induce self-excited vibration, and PZT was adhesively bonded on SMA beam to be PZT-SMA composite cantilever beam. Von de Pol item was developed to interpret the hysteresis phenomena of the strain-stress curves of SMA, and the nonlinear dynamic model of PZT-SMA composite cantilever beam subjected to stochastic excitation was obtained. The local stochastic stability of the system was analyzed according to the largest Lyapunov exponent method, and the conditions of global stochastic stability of the system were obtained in singular boundary theory. The probability density function of the dynamic response of the system was obtained, and the conditions of stochastic Hopf bifurcation were analyzed. Numerical simulation shows that self-excited vibration is induced by the hysteretic nonlinear characteristics of SMA, which can improve the efficiency of energy harvester; stochastic Hopf bifurcation appears when bifurcation parameter was adjusted, which can further increase vibration amplitude of cantilever beam system. PZT-SMA composite cantilever energy harvester combines the advantages of piezoelectric energy harvester and SMA beam, and can improve the efficiency of energy harvester obviously. The results of this paper are helpful to application of PZT-SMA composite cantilever energy harvester in engineering fields.*

1 INTRODUCTION

Piezoelectric ceramics is a kind of smart material. It can be used to convert mechanical energy into electrical energy, which is known as piezoelectric effect. Based on the effect, piezoelectric energy harvester can be designed to gather vibration energy of structures. Compared with the other types of power generation system, piezoelectric energy harvester has many advantages, such as small size, high electro-mechanical conversion efficiency, long service life, and low cost, which make it be applied as green energy widely.

Many scholars studied piezoelectric energy harvester. DuToit designed MEMS-scale piezoelectric mechanical vibration energy harvesters firstly [1]. Erturk developed the mechanical model of cantilevered piezoelectric vibration energy harvesters [2]. Priya proposed the criterion for material selection in design of bulk piezoelectric energy harvesters [3]. Liao studied parameters optimization and power characteristics of piezoelectric energy harvesters with an RC circuit [4]. In order to obtain the stable output power, piezoelectric energy harvester should be in stable periodic vibration. However, the energy of piezoelectric energy harvester was from structure vibration, which was usually random, and most of vibration energy was dissipated by the damping of the system. Usually, piezoelectric energy harvester can only provide instable or intermittent power, which limits its application in industry fields.

In this paper, a kind of PZT-SMA composite energy harvester was proposed. SMA (Shape Memory Alloy) was introduced to be the substrate of cantilever beam to induce self-excited vibration, and the stochastic bifurcation characteristics of cantilevered PZT-SMA energy harvester were analyzed.

2 HYSTERESIS NONLINEAR MODEL OF PIEZOELECTRIC ENERGY HARVESTER

The structure of cantilevered piezoelectric energy harvester was shown in Figure 1. It can be simplified as PZT-SMA cantilever beam.

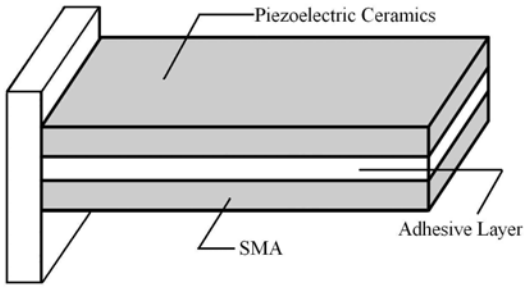

Figure 1: Structure of PZT-SMA energy harvester.

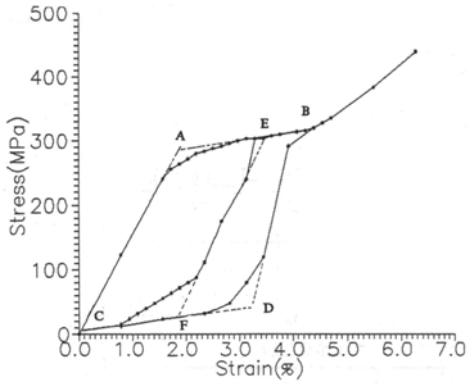

Figure 2: Strain-stress curves of SMA.

The strain-stress curves of SMA were shown in Figure 2. Obviously, there is hysteretic nonlinearity in SMA. Most of SMA models were based on thermodynamics theory and micromechanics theory, where the percentage content of martensite was taken as main variable of stress-strain equation. As results, those SMA models were mostly shown as equations with subsection function or double integral function, and hard to be analyzed in theory [5-11]. Usually, research results to those models can only be obtained by numerical method or experiment method [12-16]. In this paper, improved Von del Pol hysteretic model was introduced to describe the hysteretic nonlinear characteristics of SMA.

The initial Von del Pol hysteretic model can be shown as follows:

$$y = f(x) = f_1(x) + f_2(x) = \sum_{i=1}^{n} c_i x^i + a[1-(\frac{x}{b})^2]\dot{x} \quad (1)$$

where $f_1(x) = \sum_{i=1}^{n} c_i x^i$ is skeleton curve of hysteretic loop, which is usually expressed in polynomial function; $f_2(x) = a[1-(\frac{x}{b})^2]\dot{x}$ is Von del Pol item, which describes is the difference between the skeleton curve and the hysteretic loop; c_i, a and b are coefficients which are determined by the hysteretic loop.

The essence of Von del Pol item $f_2(x) = a[1-(\frac{x}{b})^2]\dot{x}$ are two parabolic lines which are symmetrical about the original point (0, 0), so the initial Von del Pol model can only be used in some basic parabolic hysteretic loop. However, the strain-stress curves of SMA are complex hysteretic loop which are not symmetrical about any point. In this paper, the Von del Pol hysteretic model used to describe the strain-stress curves of SMA was developed as follows:

$$\sigma = a_1\varepsilon + a_2\varepsilon^2 + a_3\varepsilon^3 + (a_4\varepsilon + a_5\varepsilon^2 + a_6\varepsilon^3 + a_7\varepsilon^4 + a_8\varepsilon^5 + a_9\varepsilon^6 + a_{10}\varepsilon^7 + a_{11}\varepsilon^8 + a_{12}\varepsilon^9 + a_{13}\varepsilon^{10})\dot{\varepsilon} \quad (2)$$

where σ is stress, ε is strain, a_i (i=1~12) are coefficients.

Partial least-square regression method was used to test the fitting effect of Eq. (2). The analyze result of principal component based on experimental data was shown in Figure 3, and the values of the coefficients were shown in Figure 4. We can see that all of the items are remarkable.

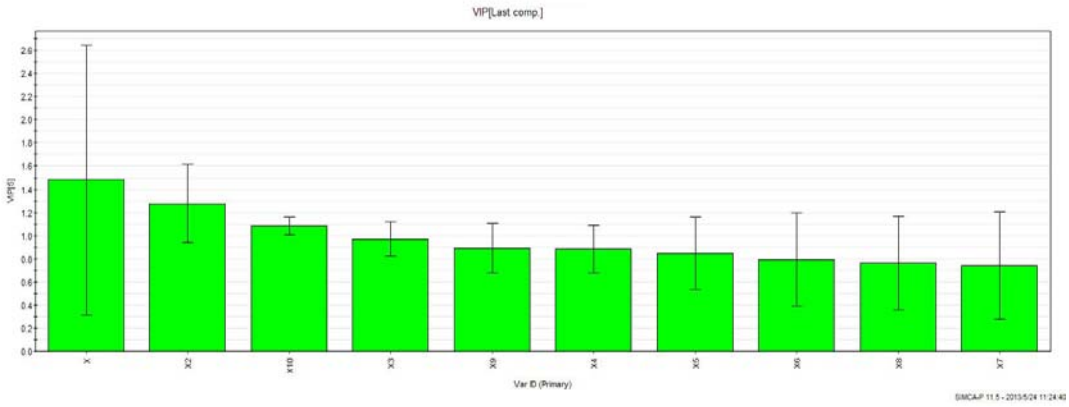

Figure 3: Analysis result of principal component.

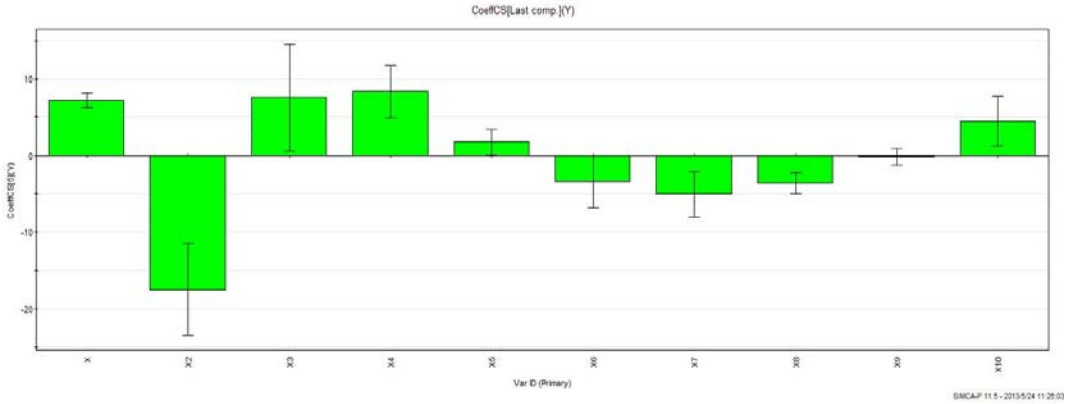

Figure 4: Values of the coefficients.

The result of forecast test to Eq. (1) was shown in Figure 5, where red line is real data and black line is forecast value. We can see that Eq. (2) can describe the real curve well.

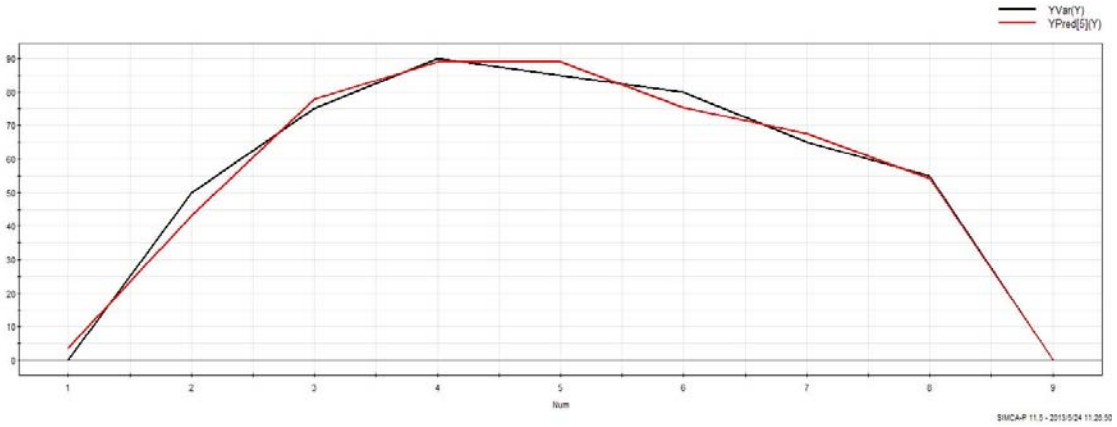

Figure 5: Results of forecast test.

The mechanical model of PZT-SMA composite energy harvester was shown in Figure 6.

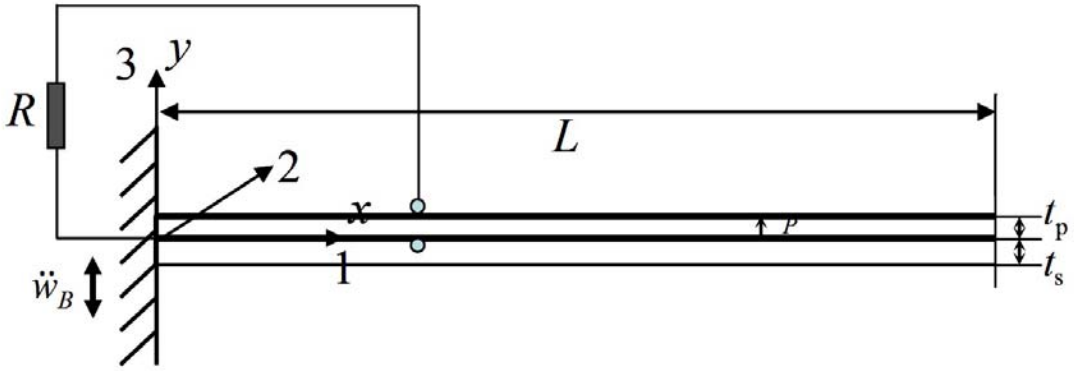

Figure 6: Mechanical model of PZT-SMA composite energy harvester.

According to Hamilton's principle, we obtained:

$$\int_{t_1}^{t_2}[\delta(T-U+W_e)+\delta W]dt=0 \tag{3}$$

where T is kinetic energy of structure, U is potential energy of structure, W_e is electric energy of piezoelectric ceramics, W is work done by external force,

$$T=\frac{1}{2}\int_{V_s}\rho_s\dot{u}^2dV_s+\frac{1}{2}\int_{V_p}\rho_p\dot{u}^2dV_p$$

$$U=\frac{1}{2}\int_{V_s}\sigma_s\varepsilon_s dV_s+\frac{1}{2}\int_{V_p}\sigma_p\varepsilon_p dV_p$$

$$W_e=\frac{1}{2}\int_{V_p}E_3D_3\mathrm{d}V_p$$

$$\delta W=\int_0^L\delta uF\,\mathrm{d}x+\delta u(l,t)F+\delta\varphi q$$

ρ_i $(i=s,p)$ is density, V_i is volume, σ_i is stress, ε_i is strain, the subscript s is SMA, p is piezoelectric ceramics; $u=u(x,t)$ is deflection of composite cantilever beam, E_3 is electric

field intensity, D_3 is electrostrictive displacement, $F = e\varsigma(t)$ is axial stochastic excitation, φ is electric potential, q is electric charge.

The constitutive model of piezoelectric ceramics can be shown as follows:

$$\begin{cases} \sigma = c_{11}^{E}\varepsilon - e_{31}E_3 - \gamma_{113}\varepsilon E_3 - \dfrac{1}{2}\beta_{133}E_3^2 + c_{111}^{E}\varepsilon^2 \\ D_3 = \varepsilon_{33}^{S}E_3 + e_{31}\varepsilon + \dfrac{1}{2}\gamma_{113}\varepsilon^2 + \beta_{133}\varepsilon E_3 + \nu_{333}E_3^2 \end{cases} \tag{4}$$

where c_{11}^{E} is stiffness coefficient, e_{31} is piezoelectric coefficient, ε_{33}^{S} is dielectric constant, γ_{113} is electroelastic coefficient, β_{133} is electrostrictive coefficient, C_{111}^{E} is nonlinear stiffness coefficient, ν_{333} is nonlinear dielectric constant.

Let $u(x,t) = \psi(x)y(t)$, the dynamic equation of piezoelectric cantilever beam subjected to axial stochastic excitation can be solved from Eq. (3) as follows:

$$\ddot{y} + 2\eta\dot{y} + \vartheta^2 U + \vartheta^2\alpha_1 yU + \frac{1}{2}\vartheta^2\alpha_2 U^2 + b_1 y + b_2 y^2 + b_3 y^3 + \dot{y}\sum_{i=1}^{10} b_{i+3}y^i = ey\varsigma(\mathrm{t}) \tag{5}$$

where y is displacement, U is voltage, η is damping, ϑ and b_i (i=1~13) are coefficients, e is intensity of stochastic excitation, $\varsigma(t)$ is Gauss white noise.

Considering that the output voltage of piezoelectric ceramics is linear with the strain, we obtain:

$$U = a_{14}d_{33}y$$

Thus, Eq. (5) can be rewritten as follows:

$$\ddot{y} + 2\eta\dot{y} + \mathrm{c}_1 y + \mathrm{c}_2 y^2 + \mathrm{c}_3 y^3 + \dot{y}\sum_{i=1}^{10} b_{i+3}y^i = \mathrm{e}y\varsigma(\mathrm{t}) \tag{6}$$

3 STOCHASTIC STABILITY OF THE SYSTEM

Let $y = q$, $\dot{y} = p$, Eq. (6) can also be shown as follows:

$$\begin{cases} \dot{q} = p \\ \dot{p} = -\mathrm{c}_1 q - \mathrm{c}_2 q^2 - \mathrm{c}_3 q^3 - (2\eta + \dot{y}\sum_{i=1}^{10} b_{i+3}y^i) + eq\varsigma(t) \end{cases} \tag{7}$$

The Hamiltonian function of Eq. (7) can be shown as follows:

$$H = \frac{1}{2}p^2 + \frac{1}{2}c_1 q^2 \tag{8}$$

According to the quasi-nonintegrable Hamiltonian system theory, the Hamiltonian function H(t) converges weakly in probability to an one-dimensional Ito diffusion process. The averaged Ito equation about the Hamiltonian function can be shown as follows:

$$dH = m(H)dt + \sigma(H)dB(t) \tag{9}$$

where $B(t)$ is standard Wiener process, $m(H)$ and $\sigma(H)$ are drift and diffusion coefficients of Ito stochastic process, which can be obtained in stochastic averaging method:

$$m(H) = (\frac{De^2}{c_1} - 2\eta)H - \frac{\sqrt{2}c_2}{3c_1}H^{\frac{3}{2}} - \frac{b_5}{2c_1}H^2 - \frac{b_7}{2c_1^2}H^3 - \frac{5b_9}{8c_1^3}H^4 - \frac{7b_{11}}{8c_1^4}H^5 - \frac{21b_{13}}{16c_1^5}H^6 \tag{10}$$

$$\sigma^2(H) = \frac{De^2}{c_1}H^2 \tag{11}$$

Based on quasi-nonintegrable Hamiltonian system theory, the largest Lyapunov exponent of a linearized system is defined as follows:

$$\lambda = \lim_{t\to\infty}\frac{1}{t}\ln H^{1/2} = \left\{m'(0) - \left[\sigma'(0)\right]^2/2\right\}/2 = \frac{De^2}{4c_1} - \eta \tag{12}$$

Now the local stochastic stability of the system can be discussed as follows:

1） The trivial solution H=0 is locally asymptotic stable if and only if $\lambda < 0$, which means $\eta > \frac{De^2}{4c_1}$;

2） The trivial solution H=0 is locally asymptotic unstable if and only if $\lambda > 0$, which means $\eta < \frac{De^2}{4c_1}$;

3） Bifurcation should appear near the trivial solution H=0 if and only if $\lambda = 0$, which means $\eta = \frac{De^2}{4c_1}$.

The largest Lyapunov exponent can only estimate the local stability. In this paper, the boundary classification method was used to analyze the global stability of the trivial solution of the system. Generally, the boundaries of diffusion process are singular, and the boundary classification is often determined by diffusion exponent, drift exponent and character value.

When $H \to 0$:

$$m(H) \to \mathrm{O}(H),\ \sigma^2(H) \to \mathrm{O}(H^2)$$

So

$$\alpha_l = 2,\ \beta_l = 1,\ c_l = 2(1 - \frac{2\eta c_1}{De^2})$$

where α_l is diffusion exponent, β_l is drift exponent, c_l is character value, l is left boundary.

Thus, the left boundary H= 0 belongs to the first kind of singular boundary. According to the classification for singular boundary , we obtained:

1）The left boundary H=0 is repulsively natural if c_l>1;

2）The left boundary H=0 is strictly natural if c_l=1;

3）The left boundary H=0 is attractively natural if c_l<1;

Similarly, the right boundary $H = \infty$ belongs to the second kind of singular boundary.

When $H \to \infty$:

$$m(H) = \mathrm{O}(H^5),\ \sigma^2(H) = \mathrm{O}(H^2)$$

So

$$\alpha_r = 2,\ \beta_r = 5,\ c_r = \frac{\sqrt{c_1}\pi b_4 - 4b_5 + 3b_6 - 2b_7}{2\sqrt{c_1}\pi De^2}$$

where r is the right boundary. Thus, the right boundary $H = \infty$ is an entrance boundary.

The necessary and sufficient conditions for globally asymptotic stability of the trivial solution require that the left boundary be attractively natural and the right boundary be entrance. Thus, the trivial solution H=0 is globally asymptotically stable only c_l <1, which means $\eta > \frac{De^2}{4c_1}$. The influence of the character value to the stability was shown in Figure 7.

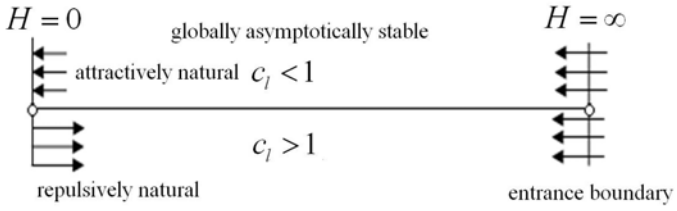

Figure 7: Influence of the character value to the stability of the system.

4 STOCHASTIC BIFURCATION AND SIMULATION

The averaged FPK equation of Eq. (8) is:

$$\frac{\partial f}{\partial t}=-\frac{\partial}{\partial H}[m(H)f]+\frac{1}{2}\frac{\partial^2[\sigma^2(H)f]}{\partial H^2} \tag{13}$$

where f is probability density.

Thus, the stationary probability density function of the system is:

$$f(H)=\overline{A}H^{-\frac{4\eta c_1}{De^2}}\exp[-\frac{4\sqrt{2}c_2}{3De^2}H^{\frac{1}{2}}-\frac{b_5}{De^2}H-\frac{b_7}{2De^2c_1}H^2-\frac{5b_9}{12De^2c_1^2}H^3-\frac{7b_{11}}{16De^2c_1^3}H^4-\frac{21b_{13}}{40De^2c_1^4}H^5] \tag{14}$$

where $\overline{A}$ is a normalization constant.

The results of numerical simulation of piezoelectric energy harvester were shown in Figure 8, where $c_1=0.5$, $D=0.5$, $\eta=0.025$, $l=1$, $M=40$, $E=2\times10^{11}$, $A=8\times10^{-4}$, $I=6\times10^{-11}$.

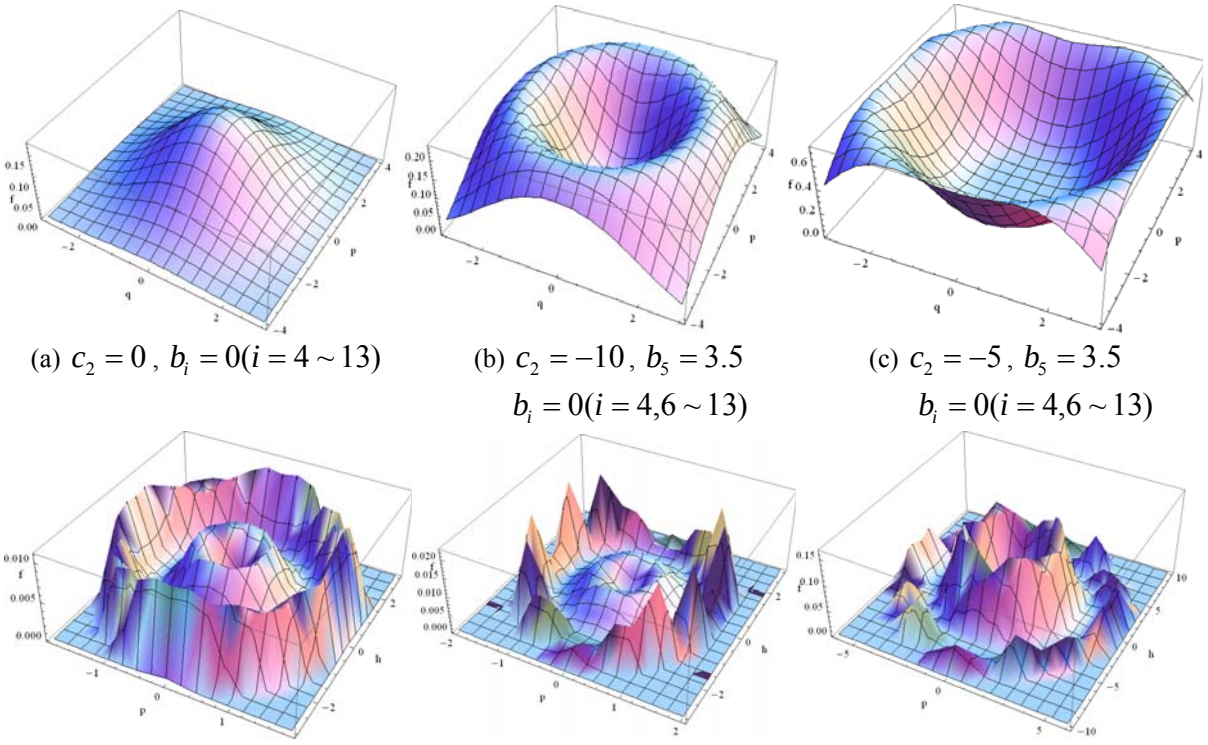

(a) $c_2=0$, $b_i=0(i=4\sim13)$ (b) $c_2=-10$, $b_5=3.5$, $b_i=0(i=4,6\sim13)$ (c) $c_2=-5$, $b_5=3.5$, $b_i=0(i=4,6\sim13)$

(d) $c_2=-5$, $b_5=3.5$, $b_7=-0.5$, $b_9=0.1$, $b_{11}=-0.01$, $b_{13}=0.00125$ (e) $c_2=-5$, $b_5=3.5$, $b_7=-1$, $b_9=0.2$, $b_{11}=-0.01$, $b_{13}=0.00125$ (f) $c_2=-10$, $b_5=3.5$, $b_7=-0.5$, $b_9=0.05$, $b_{11}=-0.01$, $b_{13}=0.00125$

Figure 8: Stationary probability density of the system response in different parameters.

From Figure 8, we can see that:

1） p=0 and q=0 when H=0, so the trivial solution H=0 corresponds to the origin (0, 0) in the figure of joint probability density;

2） To ordinary piezoelectric energy harvester, which was shown in Figure 8(a), the damping and stiffness of substrate are linear, so $c_2 = c_3 = 0$ and $b_i = 0 (i = 4 \sim 13)$. The steady-state probability density of H=0 is the max, which is locally asymptotic unstable;

3） The steady-state probability density of H=0 decreases when the system parameters c_2 and b_5 vary, which was shown in Figure 8(b) and 8(c), and its stability varies from unstable to stable. There is a limit cycle in the probability density of the system. Limit cycle means that self-excited vibration was induced by the hysteretic nonlinear characteristics of SMA, which can improve the efficiency of piezoelectric energy harvester;

4） The hysteretic nonlinear damping coefficients $b_i (i = 7,9,11,13)$ can induce Stochastic Hopf bifurcation of the system. From Figure 8(d)-8(f), we can obviously see that there are two limit cycle in the stationary probability density, which means that there are two vibration amplitudes whose probability are both very high. Jumping phenomena between the two vibration amplitudes will appear when the conditions are changed;

5） From Figure 8(d)-8(f), we can see that the stationary probability density of the response of the system can be changed through adjusting the parameters b_i. It means that different SMA materials will cause different vibration amplitudes of the system since the parameters b_i are determined by the substrate material. It provide a way to improve the efficiency of the energy harvester since the stationary probability density of the big vibration amplitude can be increased by choosing appropriate SMA material as substrate.

According to the analysis result, Fe-Mn-Si SMA and Ti-Ni SMA were chosen as substrate materials of beam independently. The experimental results of PZT-SMA composite energy harvester was shown in Figure 9 and Figure 10. We can see that the material characteristics of beam can influence the system response, and Ti-Ni SMA beam should be chosen as substrate rather than Fe-Mn-Si SMA beam.

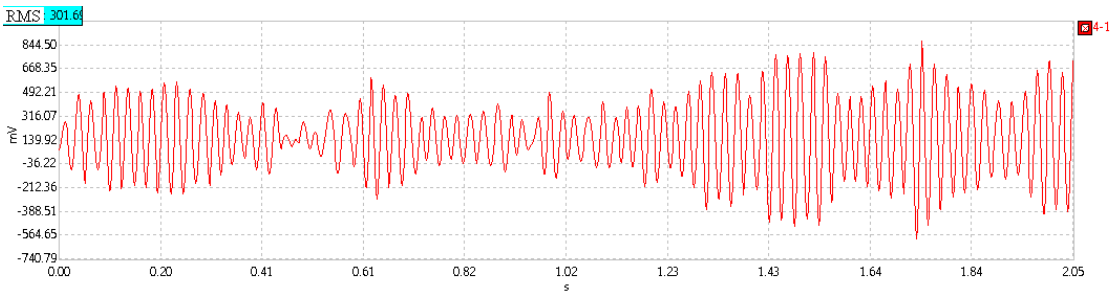

Figure 9: Response of PZT-SMA (Fe-Mn-Si) beam subjected to stochastic excitation.

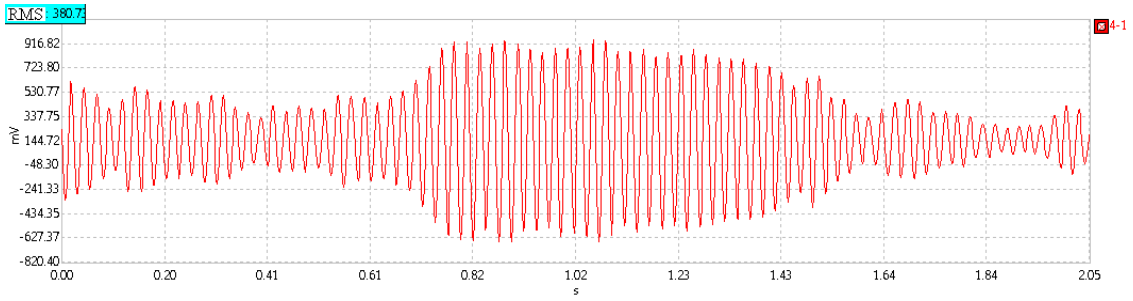

Figure 10: Response of PZT-SMA (Ti-Ni) beam subjected to stochastic excitation.

5 CONCLUSIONS

In this paper, a kind of PZT-SMA composite cantilever energy harvester was proposed, and its stochastic bifurcation characteristics were studied. SMA was chosen as the substrate of cantilever beam to induce self-excited vibration, and PZT piezoelectric ceramics was adhesively bonded on SMA beam to be PZT-SMA composite cantilever beam. Von de Pol difference item was introduced to interpret the hysteresis phenomena of the strain-stress curves of SMA, and the nonlinear dynamic model of PZT-SMA composite cantilever beam subjected to stochastic excitation was developed. The local stochastic stability of the system was analyzed according to the largest Lyapunov exponent method, and the conditions of global stochastic stability of the system were obtained in singular boundary theory. The probability density function of the dynamic response of the system was obtained, and the conditions of stochastic Hopf bifurcation were analyzed. Numerical simulation shows that self-excited vibration is induced by the hysteretic nonlinear characteristics of SMA, which can improve the efficiency of energy harvester; stochastic Hopf bifurcation appears when bifurcation parameter was adjusted, which can further increase vibration amplitude of cantilever beam system. PZT-SMA composite cantilever energy harvester combines the advantages of piezoelectric energy harvester and SMA beam, and can improve the efficiency of energy harvester obviously. The results of this paper are helpful to application of PZT-SMA composite cantilever energy harvester in engineering fields.

ACKNOWLEDGMENT

The authors gratefully acknowledge the support of Natural Science Foundation of China (NSFC) through grant no. 11272229, the Ph.D. Programs Foundation of Ministry of Education of China through grant no. 20120032120006, and Tianjin Research Program of Application Foundation and Advanced Technology through grant no. 13JCYBJC17900.

REFERENCES

[1] N. E.duToit, B. L. Wardle and S. G. Kim, Design considerations for MEMS-scale piezoelectric mechanical vibration energy harvesters. *Integrated Ferroelectrics*, **1**, 121-160, 2005.

[2] A. Erturk, D. J. Inman, On Mechanical modeling of cantilevered piezoelectric vibration energy harvesters. *Journal of Intelligent Material Systems and Structures*, **11**, 1311-1325, 2008.

[3] P. Priya, M. Shashank, Criterion for material selection in design of bulk piezoelectric energy harvesters. *IEEE Transactions on Ultrasonics Ferroelectrics and Frequency Control*, **12**, 2610-2612, 2010.

[4] Y. B. Liao, H. A. Sodano, Optimal parameters and power characteristics of piezoelectric energy harvesters with an RC circuit. *Smart Materials and Structures*, **4**, 045011, 2009.

[5] K. Tanaka, A thermomechanical sketch of shape memory effect: one-dimensional tensile behavior. *Res Mechanics*, **2**, 251-263, 1986.

[6] J. G. Boyd, D. C. Lagoudas, Thermodynamical constitutive model for shape memory materials. *International Journal of P1asticity*, **6**, 805-842, 1996.

[7] L. C. Brinson, One-dimensional constitutive behavior of shape memory alloys: thermomechanical derivation with nonconstant material functions and redefined martensite internal variable. *Journal of Intelligent Material Systems and Structures*, **2**, 229-242, 1993.

[8] E. J. Graesser, F. A. Cozzarelli, A proposed three-dimensional constitutive model for Shape memory alloys. *Journal of Intelligent Material Systems and Structures*, **1**, 78-89, 1994.

[9] Y. Ivshin, T. J. Pence, Thermomechanical model for a one variant shape memory material, *Journal of Intelligent Material Systems and Structures*, **4**, 455-473, 1994.

[10] F. Auricchio, J. Lubliner, Uniaxial model for shape-memory alloys. *International Journal of Solids and Structures*, **27**, 3601-3618, 1997.

[11] Z. W. Zhu, Q. X. Zhang, J. Xu, Nonlinear Dynamic Characteristics and Optimal Control of Giant Magnetostrictive Laminated Plate Subjected to In-plane Stochastic Excitation. *Journal of Superconductivity and Novel Magnetism*, **4**, 1343-1347, 2013.

[12] M. A. Savi, P. M. Pacheeo, M. B. Braga, Chaos in shape memory two-bar truss. *International Journal of Non-Linear Mechanics*, **8**, 1387-1395, 2002.

[13] J. W. Sohn, Y. M. Han, S. B. Choi, Vibration and position tracking control of a flexible beam using SMA wire actuators. *Journal of Vibration and Control*, **2**, 263 – 281, 2009.

[14] H. Li, Z. Q. Liu, J. P. Ou, Experimental study of a simple reinforced concrete beam temporarily strengthened by SMA wires followed by permanent strengthening with CFRP plates. *Engineering Structures*, **3**, 716-723, 2008.

[15] C. G. Wang, H. F. Tan, Experimental and numerical studies on wrinkling control of an inflated beam using SMA wires. *Smart Structures and Materials*, **10**, 1025-1031, 2010.

[16] M. S. Speicher, R. DesRoches, R. T. Leon, Experimental results of a NiTi shape memory alloy (SMA)-based recentering beam-column connection. *Engineering Structures*, **9**, 2448-2457, 2011.